Dalton Transactions

PAPER

View Article Online
View Journal | View Issue

Cite this: *Dalton Trans.*, 2017, **46**, 5297

Glycosylated metal chelators as anti-parasitic agents with tunable selectivity†

Andrew Reddy,[a] Leandro Stefano Sangenito,[b] Arthur de Azevedo Guedes,[b] Marta Helena Branquinha,[b] Kevin Kavanagh,[c] John McGinley,[d] André Luis Souza dos Santos*[b] and Trinidad Velasco-Torrijos*[a]

Received 6th December 2016,
Accepted 27th March 2017

DOI: 10.1039/c6dt04615k

rsc.li/dalton

Trypanosoma cruzi and *Leishmania amazonensis* are the causative agents of Chagas' disease and leishmaniasis, respectively. These conditions affect millions of people worldwide, especially in developing countries. As such, there is an urgent need for novel, efficient and cost-effective treatments for these diseases, given the growing resistance and side-effects of current therapies. This work details the synthesis and evaluation of the anti-parasitic activity of novel amino- and iminopyridyl metal chelators, their glycosylated derivatives and some of their metal complexes. Our results revealed the potent and metal-dependent activity for the aminopyridyl compounds: Cu(II) complexes were most effective against *T. cruzi* trypomastigotes, while Zn(II) complexes presented excellent activity against *L. amazonensis* promastigotes. In addition, the compounds showed excellent selectivity indexes and very low relative toxicity as judged by *in vitro* and *in vivo* studies, respectively, using RAW macrophages and *Galleria mellonella* larvae model.

Introduction

Neglected tropical diseases (NTD) affect in excess of 1 billion people in the most impoverished areas of the world, causing more than 500 000 deaths every year.[1] Of the major NTDs, the kinetoplastid parasite diseases leishmaniasis and Chagas disease (CD) are considered among the most challenging to tackle due to their high mortality rates and extremely limited treatment options.[2,3]

CD is a chronic, debilitating parasitic disease caused by *Trypanosoma cruzi* and is transmitted by blood-sucking insects of the subfamily *Triatominae*.[4] The disease is a significant healthcare problem and is estimated to infect more than 10 million people worldwide and presents a substantial socioeconomic burden in addition to a high morbidity rate.[1] The current treatments for CD are nifurtimox and benznidazole, both of which present undesirable side effects and limited efficacy in chronic patients.[5,6] Moreover, there is a growing resistance of *T. cruzi* towards these treatments which further necessitates novel therapeutics without cross resistance with currently used drugs.[7,8]

Leishmaniasis is a group of tropical diseases resulting from infection of parasites of the genus *Leishmania* and presents a substantial healthcare problem worldwide.[9] Leishmaniasis occurs in several forms, the most severe of which is visceral leishmaniasis (VL) which accounts for nearly 500 000 of the 2 million cases of leishmaniasis reported annually and is fatal if left untreated.[10] VL is caused by the infection of the host's macrophages with *Leishmania* amastigotes following infection with promastigotes which are transmitted by the female sand fly.[11] First line treatment typically employs pentavalent antimonials such as sodium stibogluconate. However, there is widespread resistance to these compounds which leads to the use of amphotericin B as the preferred treatment for VL.[12–14] Unfortunately, the use of this drug in endemic regions is limited by its cost, toxicity and difficulties of administration.[15] These challenges demonstrate the urgent need for novel, safe and cost-effective therapies for these diseases. In particular, drugs with activity against multiple kinetoplastid parasites are especially attractive due to their broad spectrum of activity.[16]

Metallodrugs are an emerging therapeutic approach in the treatment of parasitic diseases.[17,18] Accordingly, several metal complexes have been investigated against CD and leishmaniasis.[4,19–21] The combination of metal ions with drugs and organic ligands can enhance their activity while at the same time, reducing the toxicity and undesired side effects that metal ions on their own could impart.[22–24]

[a]*Department of Chemistry, Maynooth University, Maynooth, Co. Kildare, Ireland. E-mail: trinidad.velascotorrijos@nuim.ie*
[b]*Department of General Microbiology, Microbiology Institute Paulo de Góes, Federal University of Rio de Janeiro (UFRJ), Rio de Janeiro, RJ, 21941-590, Brazil. E-mail: andre@micro.ufrj.br*
[c]*Department of Biology, Maynooth University, Maynooth, Co. Kildare, Ireland*
[d]*Department of Chemistry, University of Copenhagen, DK-2100 Copenhagen, Denmark*

†Electronic supplementary information (ESI) available. CCDC 1518825–1518827 and 1518829. For ESI and crystallographic data in CIF or other electronic format see DOI: 10.1039/c6dt04615k

In this study, the synthesis of a series of amino- and iminopyridyl ligands and some of their metal complexes is reported. In addition, their anti-parasitic activity against *L. amazonensis* promastigotes and *T. cruzi* trypomastigotes is evaluated. With a view to further improve their selectivity and bioavailability, the synthesis and assessment of the anti-parasitic activity of some per-acetylated glucosyl analogues has also been performed. Carbohydrate conjugation is an attractive means of improving the selectivity of bioactive molecules through a targeting strategy.[25,26] However, the water-soluble character of saccharides can compromise their ability to cross cellular membranes. Therefore, the use of acetylated sugars, with increased hydrophobicity, which undergo hydrolysis after administration is often preferred.[27] Thus, the glycosylation of metal chelators seems a logical approach to enhance their therapeutic potential.[28]

Results and discussion

Synthesis

The synthesis of the aminopyridyl ligands **2a**[29] and **2b** (N_2 series, Scheme 1a) was achieved by the reductive amination of aldehydes **1a** and **1b**,[30] respectively. The reduction of the corresponding imines was carried out *in situ* since they were found to be very sensitive to hydrolysis. The metal complexes studied were obtained by the direct reaction of ethanolic solutions of the ligands and metal salts. Complexes with Cu(II) (1 : 1 complexes **3a** and **3b**) were formed from ligands **2a** and **2b**, while the complex of **2a** with Zn(II) was formed in a 2 : 1 stoichiometry (complex **4**).

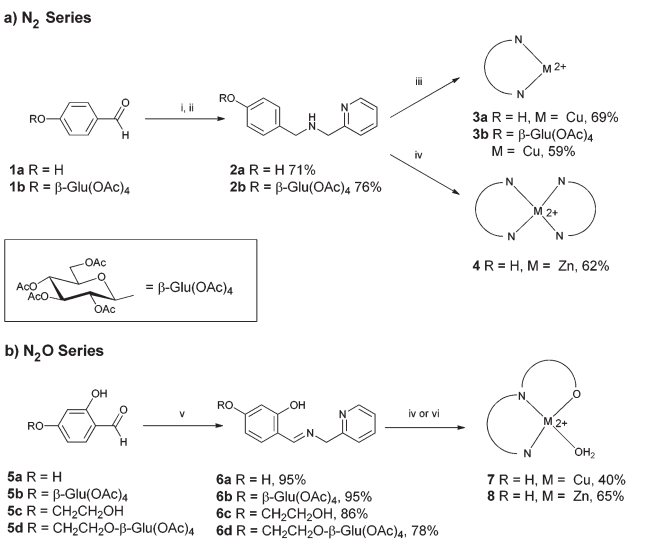

Scheme 1 Synthesis of (a) aminopyridyl ligands (N_2 series) and (b) iminopyridyl (N_2O series) ligands and some of their metal complexes. Reagents and conditions: (i) 2-picolylamine, ethanol, $MgSO_4$, 80 °C, 4 h; (ii) $NaBH_4$, ethanol/acetic acid, −10 °C to rt, 16 h; (iii) $CuCl_2{\cdot}2H_2O$, ethanol, rt, 16 h; (iv) $Zn(ClO_4)_2{\cdot}6H_2O$, ethanol, rt; (v) 2-picolylamine, ethanol, rt, 4–6 h; (vi) $Cu(ClO_4)_2{\cdot}2H_2O$, ethanol, 5 h.

Crystals suitable for X-ray crystallography of **3a** were obtained from a solution of the complex in acetonitrile. This was found to contain two distinct 5-coordinate Cu(II) species; an acetonitrile adduct $[Cu(\mathbf{2a})(CH_3CN)Cl_2]$ (Fig. 1A) encapsulated inside a unit cell with a binuclear bridged species $[Cu_2(\mathbf{2a})_2Cl_2(\mu_2\text{-}Cl)_2]$ (Fig. 1B) occupying the vertices (see also ESI-1.1†).

In the mononuclear species, the ligand **2a** is coordinated in a bidentate fashion with a bite angle of 82.60°. The Cu–N_{pyr} and Cu–N_{amine} are bonded at distances of 2.025 Å and 2.046 Å respectively, while acetonitrile adduct shows a Cu–N_{MeCN} bond length of 2.302 Å.

The chloride ligands are coordinated symmetrically with Cu–Cl bonds of 2.313 Å. The structure has a τ_5 value of 0.07 corresponding to a square pyramidal geometry.[31] There is a short range interaction of 3 Å between the Cu(II) coordination centre and a chloride ligand of a neighbouring molecule.

The dimer on the other hand shows a bond length of 2.257 Å for the axial Cu–Cl bond while the bridging Cu–Cl bonds are asymmetrically elongated with lengths of 2.302 Å and 2.692 Å. **2a** binds more tightly to the metal centre compared to the mononuclear complex with lengths of 2.010 Å and 2.036 Å for the Cu–N_{pyr} and Cu–N_{amine} interactions and a slightly smaller bite angle of 82.25°. This molecule has a τ_5 value of 0.15 which indicates a higher degree of distortion from the ideal square pyramidal geometry than the mononuclear acetonitrile adduct described above. As the elemental analysis of the compound indicates the presence of a water molecule, it is likely that the material obtained is a 5-coordinate complex analogous to the acetonitrile adduct with water occupying the axial position in place of the acetonitrile ligand.

We examined the stability of the Cu(II) complex **3a** by recording UV/Vis spectra of a solution of **3a** in DMSO/water a 0 h, 24 h and 72 h. No appreciable changes were observed (Fig. 2.1-ESI†). We also examined the stability of the Zn(II) complex **4** by recording ^{1}H NMR spectra of a solution of **4** in d_6-DMSO/D_2O a 0 h and 72 h (Fig. 2.2-ESI†) and again, no appreciable changes were observed.

Contrary to the N_2 compounds, the imine ligands corresponding to the N_2O series (Scheme 1b) were readily prepared

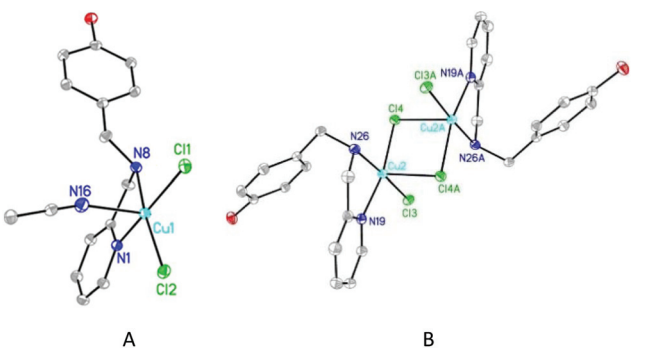

Fig. 1 X-ray crystal structures of **3a** with atomic displacement parameters shown at 50% probability. Hydrogen atoms omitted for clarity.

by the direct reaction of 2-picolylamine with aldehydes **5a–d** without the need for acid catalysis or desiccating agents. The presence of the *ortho* hydroxyl group provides a favourable hydrogen bond interaction with the imine lone pair of electrons which results in the shifting of the ^{1}H NMR resonance of the *ortho* phenolic protons of imines **6b–d** to 13–14 ppm from 11.4 ppm in the precursor aldehydes. This hydrogen bonding is also observed in the crystal structures of **6a** and **6c** (ESI-1.2 and 1.3†) and confers an unusual stability on these imines and a remarkable resistance to hydrolysis, even when stored under ambient conditions.

Preliminary investigations into the optimum experimental conditions for the synthesis of metal complexes with ligands of the N_2O series focused on those for ligand **6a**. The Cu(II) and Zn(II) complexes, **7** and **8**, respectively, presented a 1 : 1 stoichiometry. However, it was observed by NMR spectroscopy that Zn(II) complex **8** was unstable in solution and hydrolyzes to the aldehyde **5a** and the bis(2-picolylamine)zinc perchlorate complex **9**. The identity of this compound was confirmed by NMR and X-ray crystallography of the crystals obtained from the NMR sample of **8** in d_8-THF (Fig. 2, see also ESI-1.4†). Interestingly, this adopts an unusual coordination geometry with a τ'_4 value of 0.70 which suggests a distorted see-saw structure (τ'_4: 0.64). This is consistent with previously reported see-saw structures which exhibit τ'_4 values of 0.70 ± 0.02.[32,33] This geometry has only been reported once in the literature for a zinc compound which contained Zn(0)[34] and, to the best of our knowledge, it has not been yet reported for a Zn(II) complex. Complex **9** can also be synthesized by the direct reaction of 2-picolyamine and $Zn(ClO_4)_2{\cdot}6H_2O$. The NMR data of the hydrolysis product was identical to that of the complex **9** synthesized purposely. The analogous Cu(II) complex **7** exhibits a much greater stability in solution at room temperature. However, the corresponding Cu(II) picolylamine complex $[Cu(2\text{-picolylamine})_2(ClO_4)_2]$[35] can be formed by refluxing the complex **7** for 24 h in ethanol, causing the hydrolysis of the ligand. The 2-picolylamine ligands in the Cu(II) picolylamine complex were reported to coordinate in an *anti* fashion while crystallographic data showed the ligands in Zn(II) complex **9** binding in a *syn* manner.

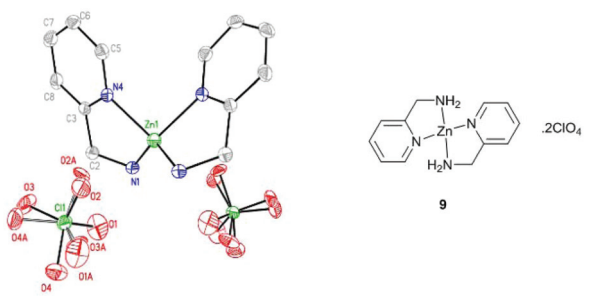

Fig. 2 Molecular structure of **9** with atomic displacement parameters shown at 50% probability. Hydrogen atoms omitted for clarity. Only symmetry unique atoms are labelled. Perchlorate oxygen atoms are modelled in two positions with occupancies of 69/31%.

Evaluation of *in vitro* cytotoxicity to macrophage cells

A library of eleven compounds (Fig. 3) was initially screened to test the cytotoxicity of the compounds. They were administered to murine macrophages and their viability was estimated using the MTT assay in order to determine the cytotoxicity concentration (CC_{50}). The simple metal salts $CuCl_2{\cdot}2H_2O$ and $ZnCl_2$ did not show significant toxicity, with activities comparable to the control. All of the compounds exhibited low toxicity towards RAW cells (Fig. 3.1-ESI†) with complex **3a** presenting the highest toxicity (106.2 μM). In contrast, the least toxic compound was Zn(II) complex **8** which exhibited a CC_{50} above the highest concentration used (400 μM); however, given that this compound was found to hydrolyze in DMSO, it is likely that any activity observed is due to the hydrolysis products. These data suggests that both amino- and iminopyridyl derivatives are well tolerated by mammalian cells.

Anti-*T. cruzi* activity

The anti-parasitic activity of the ligands and their metal complexes was then evaluated. The library of compounds was initially screened for inhibitory activity against the viability of *T. cruzi* trypomastigotes at a concentration of 50 μM. Seven compounds (**2a–b**, **3a–b**, **4**, **6b**, **7**) significantly reduced the viability of *T. cruzi* (Fig. 4A). The simple metal salts $CuCl_2{\cdot}2H_2O$ and $ZnCl_2$ showed similar activity to the control. All members of the N_2 series showed activity, while from the N_2O series,

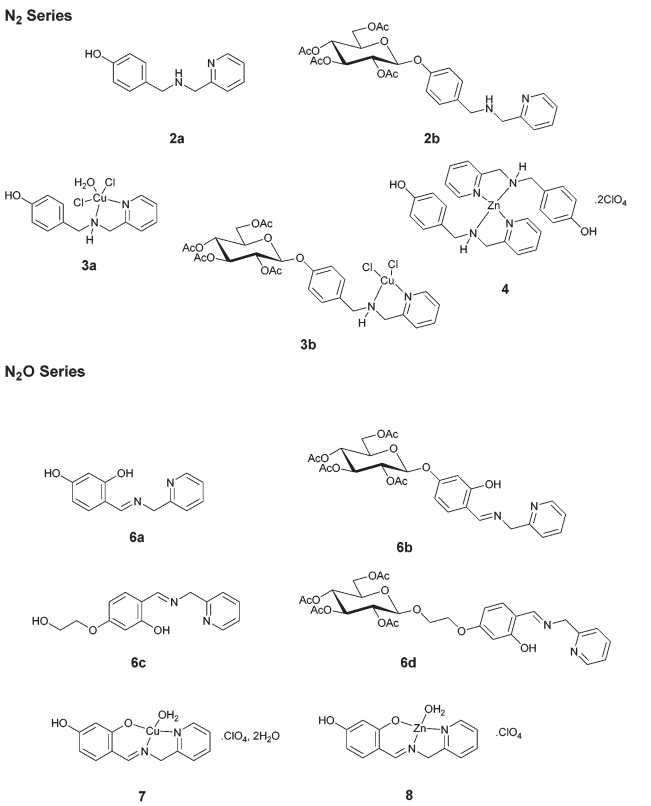

Fig. 3 Chemical structure of the amino- and iminopyridyl ligands and metal complexes evaluated for anti-parasitic activity.

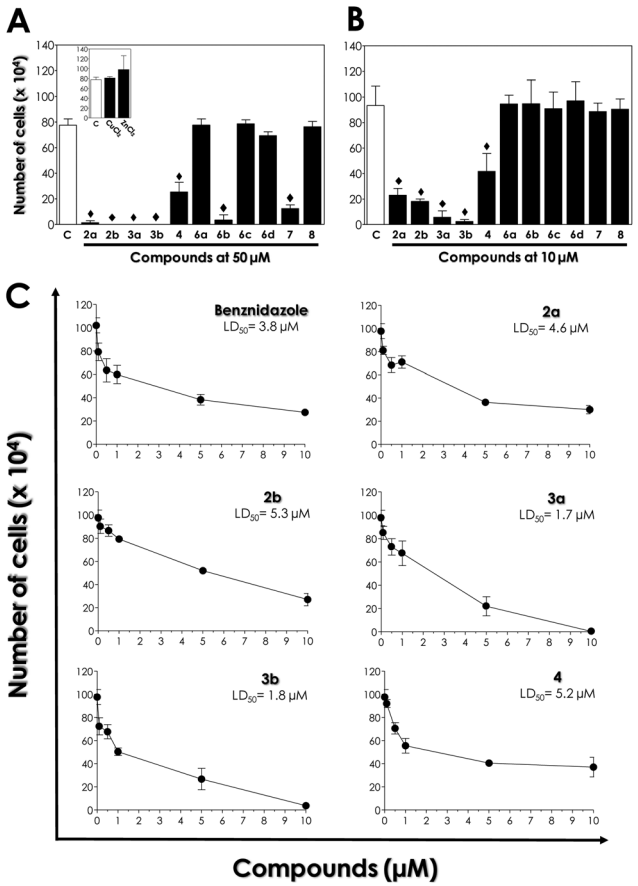

Fig. 4 Effects of amino/iminopyridyl derivatives on the viability of *T. cruzi* trypomastigotes. (A) Viability rate of trypomastigotes (initial inoculum of 10^6 cells per mL) at 37 °C in absence/presence of the compounds (50 µM). The parasites were counted 24 h after addition of the compounds; inset: control with the simple Cu(II) and Zn(II) salts. (B) Compounds screened at 10 µM as described in A. (C) Cell death profile with selected compounds at appropriated concentrations (0.1 to 10 µM). The viable parasites were counted by Trypan blue exclusion and motility in a Neubauer chamber after 24 h of incubation. Benznidazole was used as a positive control. Results are expressed as number of viable cells. DMSO (solvent used), was used as a control and did not affect the parasite viability (data not shown). Data shown are the mean ± standard deviation of three independent experiments performed in triplicate. The symbols represent the significant differences in relation to the control ($P < 0.01$).

only the glycosylated ligand **6b** and the Cu(II) complex **7** were active. All of the compounds were then tested at 10 µM (Fig. 4B) and the LD_{50} values of the most active compounds were determined (Fig. 4C and Table 1). The Cu(II) complexes **3a–b** (LD_{50} values of 1.7 and 1.8 µM, respectively) showed significantly better efficacy than the current clinical drug benznidazole (LD_{50} value 3.8 µM) towards *T. cruzi*, while the non metallated ligands **2a–b** and the Zn(II) complex **4** (LD_{50} values 4.6, 5.3, 5.2 µM, respectively) showed comparable activity.

The effect of the active compounds on the morphology of *T. cruzi* was then evaluated. Compounds from the N_2 series (**2a–b**, **3a–b**, **4**) were administered to the parasite at their LD_{50} concentrations and cell morphology was inspected by means of optical microscopy after 24 h exposure (Fig. 5). Non-treated trypomastigote cells retained their typical elongated shape, in which the flagellum is attached along the length of the para-

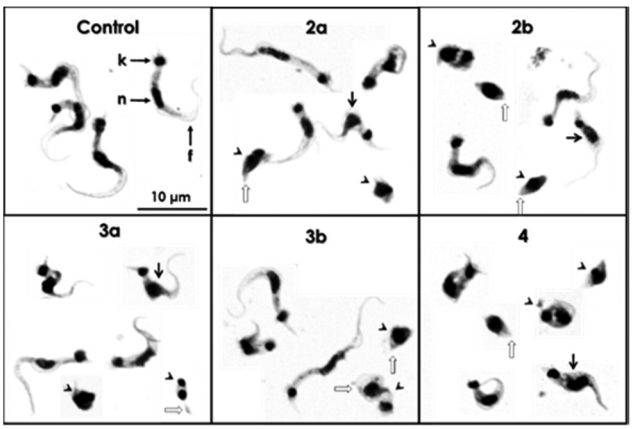

Fig. 5 Effect of selected compounds on the morphology of *T. cruzi* trypomastigotes. Giemsa-stained smears of trypomastigotes were prepared after incubation in the presence of each compound at LD_{50} concentration for 24 h. Non-treated trypomastigotes (control) present a kinetoplast (k), a central nucleus (n) and a flagellum (f) attached to the parasite cell body. Compound administration induced numerous morphological changes, such as parasites becoming round in shape with reduced cell size (arrowhead), swelling of the cell body (black thin arrow), and shortening or loss of flagellum (white arrow). All images are shown in the same scale (bar = 10 µm).

Table 1 Selectivity indexes (SI) of compounds exhibiting the highest anti-parasitic activity

	RAW CC_{50}	*T. cruzi* LD_{50}	*L. amazonensis* IC_{50}	RAW/*T. cruzi*	RAW/*L. amazonensis*
Compd	[µM]			SI	
2a	155.4	4.6	25.3	33.8	6.1
2b	234.5	5.3	7.1	44.2	33
3a	106.2	1.7	—	62.5	—
3b	127.6	1.8	—	70.9	—
4	118.2	5.2	1.3	22.7	90.9
6b	196.1	—	18.4	—	10.7
8	>400	—	17.1	—	>23.4
Benznidazole	182.1	3.8	—	47.9	—
Amphotericin B	37.4	—	0.012	—	3.116

site cell body, with an undulating membrane provided by flagellum movement and an unaltered surface. The treatment of trypomastigotes with the test compounds caused some significant morphological changes when compared to the typical appearance of non-treated parasites, including rounding in shape with reduced cell size, swelling of the cell body and shortening or loss of flagellum (Fig. 5).

Anti-*L. amazonensis* activity

The ability of the compounds to inhibit the proliferation of *L. amazonensis* promastigotes was then evaluated. Firstly, the compounds were screened at initial concentrations of 50 and 10 μM, respectively (Fig. 6A and B). Only compounds **2a–b**, **4**, **6b** and **8** showed inhibitory effects on promastigote proliferation. The Zn(II) complex **4** from the N_2 ligand series had the highest activity, whilst the hydrolysis products of Zn(II) complex **8** had comparable activity to those of the glycosylated ligands **2b** and **6b**. As observed in the previously discussed biological assays, the simple metal salts $CuCl_2{\cdot}2H_2O$ and $ZnCl_2$ had no anti-parasitic effect. The five most active compounds were then tested across a range of concentrations to establish the IC_{50} values (Fig. 6C and Table 1). All the compounds showed dose-dependent activities: the activity of free ligand **2a** (IC_{50} = 25.3 μM) was greatly enhanced by the presence of Zn(II) in complex **4** (IC_{50} = 1.3 μM) and, to a lesser extent, by conjugation to glucose, as evidenced by activity of **2b** (IC_{50} = 7.1 μM). On the other hand, the compounds from the N_2O series showed similar activities, with IC_{50} values of 17.1 μM for the hydrolysis products of Zn(II) complex **8** and 18.4 μM for glycosylated ligand **6b**. These results highlight the potential for development of the active compounds, especially when considering the severe toxicity of current treatments for leishmaniasis.

As with *T. cruzi*, the *L. amazonensis* parasites were inspected using light microscopy 72 h after the administration of each compound at its IC_{50} value (Fig. 7). Untreated promastigotes exhibited their typical elongated shape with a long flagellum emerging at the anterior end of the parasite. The treated parasites displayed significant changes to their morphology when compared to these control cells. These changes include loss of flagellum and a reduced cell size. Further morphological alterations, such as a swelling and rounding of the cell, were also observed.

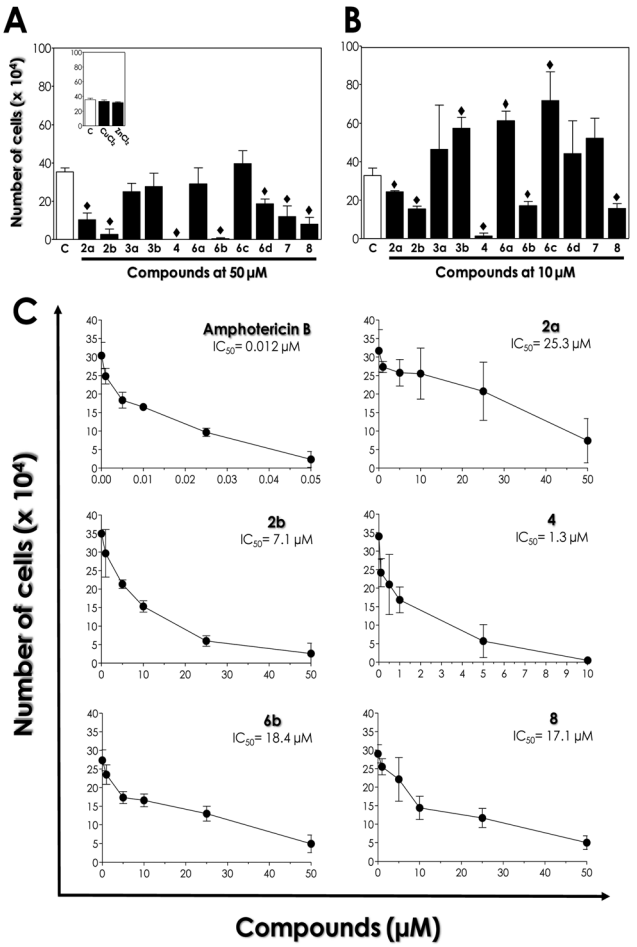

Fig. 6 Effects of amino/iminopyridyl derivatives on the proliferative rate of *L. amazonensis* promastigotes. (A) The proliferation of promastigotes (initial inoculum of 10^5 cells per mL) was followed at 28 °C in absence/presence of the compounds (50 μM). The parasites were counted 72 h after addition of the compounds; inset: control with the simple Cu(II) and Zn(II) salts. (B) Compounds screened at 10 μM as described in (A). (C) Cell proliferation profile with selected compounds at appropriated concentrations (0.1 to 50 μM). The viable parasites were counted by Trypan blue exclusion and motility in a Neubauer chamber after 72 h of incubation. Amphotericin B was used as a positive control. Results are expressed as number of viable cells. DMSO (solvent used), was used as a control and did not affect the parasite viability (data not shown). Data shown are the mean ± standard deviation of three independent experiments performed in triplicate. The symbols represent the significant differences in relation to the control ($P < 0.01$).

Evaluation of *in vivo* cytotoxicity to *Galleria mellonella* larvae

The active compounds **2a–b**, **3a–b**, **4**, **6a–b** and **8** were also screened for toxicity against larvae of *G. mellonella*, a model organism used as a surrogate to probe the response of the human innate immune system.[36–39] Compounds were administered at concentrations of 1, 10 and 100 μM and the viability of the larvae was assessed at 24 and 48 h. All of the larvae treated with the compounds survived and none of those displayed any melanization of their cuticle, which is indicative of an immune response (Fig. 3.2-ESI†).

Overall, these results indicate that the compounds from the N_2 series (aminopyridyl derivatives) are more effective antiparasitic agents than their corresponding iminopyridyl derivatives (N_2O series). Considering the anti-*T. cruzi* activities, the selectivity indexes for the Cu(II) complexes **3a–b** (62.5 and 70.9, respectively, Table 1) are significantly higher than that for reference drug benznidazole (47.9), currently used in the treatment for CD. Other Cu(II) complexes with known drugs, like risedronate or levofloxacin[40,41] present IC_{50} values as low as 1.6 μM, however the corresponding selectivity indexes were as high as 19.[4] While there are some examples of Cu(II) complexes capable of inhibiting the growth of *T. cruzi*,[24,40–43] our results represent a marked improvement in the development of selec-

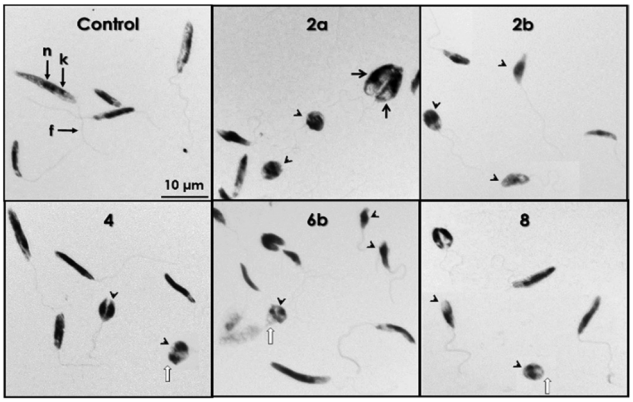

Fig. 7 Effect of selected compounds on the morphology of *L. amazonesis*. Giemsa-stained smears of promastigotes were prepared after incubation in the presence of each compound at LD_{50} concentration for 72 h. Non-treated promastigotes (control) present a kinetoplast (k), a central nucleus (n) and a flagellum (f) attached to the parasite cell body. The treatment induced morphological changes, such as parasites becoming round in shape with/or reduced cell size (arrowhead), swelling of the cell body (black thin arrow) and loss of flagellum (white arrow). All images are shown in the same scale (bar = 10 μm).

tive Cu(II)-based therapies for CD. It seems clear that Cu(II) coordination enhances the anti-parasitic activity of the ligands: a reduction in the IC_{50} value of the free ligand **2a** from 4.6 μM to 1.7 μM for complex **3a** was observed (a 2.7-fold decrease); the glucosylated ligand **2b** presents an IC_{50} value of 5.3 μM while the corresponding Cu(II) complex **3b** has 1.8 μM (a 2.9-fold decrease). This moderate improvement in the activity suggests that metal complexation does not prompt the synergistic effects as reported for some anti-trypanosomal complexes. These effects are characterized by a dramatic increase in ligand activity upon metal coordination.[23] In our case it seems more likely that Cu(II) provides additional affinity for the target binding site(s), which would explain the slight increase in activity compared to the ligands on their own. The Zn(II) complex **4**, with a 2 : 1 stoichiometry, possesses coordination environment and molecular geometry rather different to the Cu(II) complexes, which may not be so favourable for binding with the target and could therefore account for the reduced activity (5.2 μM). Some of the anti-trypanosomal Cu(II) complexes reported in the literature bind to DNA, which could lead to their anti-parasitic activity.[41,42] A common structural feature of these is the presence of a dinitrogen chelating motif, such as 1,10-phenanthroline and 2,2′-bipyridine, which are known cytotoxic agents.[41–44] However, the compounds described herein lack the extended aromatic planar surfaces required for efficient DNA intercalation. The high tolerance of the N_2 ligand scaffolds, as evidenced by their high selectivity indexes (Table 1) and the *G. mellonella* assays suggest that, from a structural perspective, the compounds are not likely to effect high affinity DNA binding. However, further studies would be necessary in order to determine their mechanism of action.

The influence of the coordinated metal in the anti-parasitic activities is more evident considering the results from the anti-leishmanial assays. In this case, none of the Cu(II) complexes evaluated was able to inhibit the proliferation of *L. amazonensis* promastigotes. On the other hand, the Zn(II) complex **4** showed a remarkably low IC_{50} value of 5.2 μM together with a selectivity index of 90.9. Zn(II) species have been used to treat cutaneous leishmaniasis as both nutritional supplements and topical drugs.[45,46] Zn(II) complexes featuring the 2-picolylamine binding motif have been recently reported to inhibit the growth of *L. major*, with good activity *in vivo*.[47] We found that the hydrolysis products from complex **8**, namely Zn(II) complex **9**, also showed anti-parasitic activity to some extent (17.1 μM). Several modes of action for Zn(II) complexes with anti-leishmanial properties have been discussed in the literature: some compounds have been reported to inhibit enzymes essential for the parasite's carbohydrate metabolism, such as those involved in the Embden–Meyerhof pathway.[48] Some studies have indicated that Zn(II) complexes selectively recognize anionic cell surfaces through a combination of electrostatic attraction and specific coordination of the zinc cations with phospholipids in the cell membrane.[49,50] Given the changes in parasite morphology effected by the Zn(II) complexes described herein resulting in loss of the distinct shape of the parasite, a structural component of the parasite membrane could be proposed as a plausible target. However, in depth studies, including TEM imaging, are necessary in order to ascertain this hypothesis. It should be also noted that glucosylated ligands **2b** and **6b** showed significant anti-leishmanial activities (7.1 μM and 18.4 μM, respectively). The mechanism of action of these ligands maybe multifunctional, and further investigations are required in order to elucidate it. Finally, compounds **6c**, in which the phenolic hydroxyl has been alkylated and **6d**, its glucosylated analogue, showed low activity against both of the parasites studied in this work. This highlights the importance of the phenolic glycoside structural feature for the biological activity of the compounds, suggesting that only glycosylated compounds susceptible to the action of glucosidases would show anti-parasitic activity.

Conclusions

In summary, a collection of amino- (N_2) and iminopyridyl (N_2O) ligands, their glucosylated analogues and some of their divalent metal complexes have been synthesized and their anti-parasitic activity towards *T. cruzi* and *L. amazonensis* evaluated. The compounds from the N_2 series were found to be more active than their corresponding N_2O analogues. The nature of the metal ion strongly influences the biological activities of the complexes investigated: Cu(II) complexes **3a** and **3b** showed potent activity against *T. cruzi* while the Zn(II) complex **4** was most efficient at inhibiting the growth of *L. amazonensis*. Moreover, the most potent compounds presented remarkable selectivity indexes; in particular, the anti-trypanosomal compounds were considerably higher than the control drug currently in use for the treatment of CD. These preliminary studies suggest that these compounds could be

extremely attractive candidates for further development as novel anti-kinetoplastid therapeutic agents.

Experimental

Chemistry general methods

All chemicals purchased were reagent grade and used without further purification unless stated otherwise. Dichloromethane and acetonitrile were freshly distilled over CaH_2 prior use. Ethanol was dried over 3 Å molecular sieves, which were flame dried, prior to use. Reactions were monitored with thin layer chromatography (TLC) on Merck Silica Gel F_{254} plates. Detection was effected by UV or charring in a mixture of 5% sulfuric acid–ethanol. All glassware used for anhydrous reactions was flame dried under vacuum prior to use. NMR spectra were obtained on a Bruker Ascend 500 using the residual solvent peak as internal standard. Chemical shifts are reported in ppm. Flash chromatography was performed with Merck Silica Gel 60. Microwave reactions were carried out using a CEM Discover Microwave Synthesizer. Optical rotations were obtained from an AA-100 polarimeter. $[\alpha]_D$ values are given in 10^{-1} cm^2 g^{-1}. The melting points were obtained using a Stuart Scientific SMP1 melting point apparatus and are uncorrected. Purity was confirmed by elemental analysis using a FLASH EA 1112 Series Elemental Analyzer with Eager 300 operating software. High resolution mass spectrometry (HRMS) was performed on an Agilent-LC 1200 Series coupled to a 6210 Agilent Time-Of-Flight (TOF) mass spectrometer equipped with an electrospray source in both positive and negative (ESI+/−) modes. Magnetic susceptibility measurements were carried out at rt using a Johnson Matthey Magnetic Susceptibility Balance with $[HgCo(SCN)_4]$ as reference. Infrared spectra were obtained as a film on NaCl plates or as KBr disks in the region 4000–400 cm^{-1} on a PerkinElmer Spectrum 100 FT-IR spectrophotometer. Purity of tested compounds was 95% or higher, as determined by elemental analysis (results within 0.4% of theoretical values). **Caution**: Although not encountered in our experiments, perchlorate salts of metal ions are potentially explosive and should be manipulated with care.

Synthesis

Compounds **1b**,[30] **2a**,[29] **5b**,[51] **5c**[52] have been previously reported. For optimized synthetic procedures and complete characterization, see ESI.†

***N*-{[4-(2,3,4,6-Tetra-*O*-acetyl-β-D-glucopyranosyloxy)phenyl]methyl}-2-pyridinemethamine (2b).** **1b** (1 g, 2.2 mmol) and 2-picolylamine (0.24 mL, 2.2 mmol) were stirred in ethanol (25 mL) with anhydrous $MgSO_4$ (0.8 g, 6.6 mmol) at 80 °C for 4 h under a nitrogen atmosphere. The mixture was filtered and cooled to −10 °C in an ice/acetone/NaCl bath under nitrogen. Acetic acid (0.12 mL, 2.2 mmol) was added immediately followed by the dropwise addition of a solution of sodium borohydride (0.33 g, 8.8 mmol) in ethanol (30 mL). The solution was allowed to warm to rt and was stirred for 16 h before being quenched by the addition of water (20 mL). The mixture was heated to 80 °C for 30 min until the precipitation of boron salts ceased. The precipitate was removed by filtration and the filtrate was evaporated under reduced pressure. The resulting residue was dissolved in water (20 mL) and aq. $NaHCO_3$ saturated solution (30 mL) was added to adjust the pH to approximately 9. It was then extracted with ethyl acetate (5 × 40 mL). The combined organic layers were washed with brine (100 mL), dried (Na_2SO_4) and the solvent was removed *in vacuo*: brown syrup (0.91 g, 76%); ^{1}H NMR (500 MHz, $CDCl_3$) δ 8.51 (d, J = 4.5 Hz, 1H, Pyr-H), 7.60 (t, J = 7.6 Hz, 1H, Pyr-H), 7.27–7.23 (m, 3H, Pyr-H, Ar–H), 7.15–7.11 (m, 1H, Pyr-H), 6.91 (d, J = 8.4 Hz, 2H, Ar–H), 5.24 (m, 2H, H-2, H-4), 5.12 (t, J = 9.3 Hz, 1H, H-3), 5.02 (d, J = 7.1 Hz, 1H, H-1), 4.24 (dd, J = 12.4, 5.3 Hz, 1H, H-6), 4.13 (dd, J = 12.4, 2.0 Hz, 1H, H-6′), 3.87 (s, 2H, $PyrCH_2$), 3.81 (ddd, J = 7.6, 5.3, 2.0 Hz, 1H, H-5), 3.76 (s, 2H, $ArCH_2$), 2.94 (bs, 1H, N–H), 2.03, 2.02, 2.00, 1.99 (each s, 3H, OAc). ^{13}C NMR (126 MHz, $CDCl_3$) δ 170.7, 170.4, 169.5, 169.4 (each C=O), 159.5 (Pyr-C), 156.2 (Ar–C), 149.4 (Pyr-CH), 136.6 (Pyr-CH), 129.7 (Ar–C), 128.6 (Ar–CH), 122.6 (Pyr-CH), 122.2 (Pyr-CH), 117.2 (Ar–CH), 99.5 (C-1), 72.9 (C-4), 72.2 (C-5), 71.4 (C-3), 68.5 (C-2), 62.1 (C-6), 54.3 ($PyrCH_2$), 52.8 ($ArCH_2$), 20.85, 20.82, 20.77, 20.75 (each OAc). IR (film on NaCl): 3427, 2945, 3922, 1751, 1610, 1592, 1511, 1474, 1435, 1369, 1214, 1069, 1042, 908, 831, 761, 600 cm^{-1}. HRMS (ESI$^+$): m/z calculated for $C_{27}H_{32}N_2O_{10}$ + H^+ [M + H^+]: 545.2135. Found: 545.2139. $[\alpha]_D^{22}$: −0.07 (c 0.5, dichloromethane). Elemental analysis calculated (%) for $C_{27}H_{32}N_2O_2$: C 59.55, H 5.92, N 5.14. Found: C 59.27, H 6.10, N 5.03.

***cis*-Aquadichloro(*N*-[4-(hydroxyphenyl)methyl]-2-pyridinemethamino)copper (3a).** Compound **2a** (438 mg, 2 mmol) was dissolved in ethanol (10 mL) and was added to a solution of $CuCl_2{\cdot}2H_2O$ (348 mg, 2 mmol) in ethanol (15 mL). A green precipitate was formed and the reaction was allowed to stir at rt overnight. The solvent was reduced by half *in vacuo* and was then cooled on ice for 30 min and a green solid was collected by vacuum filtration. This was washed with cold ethanol and dried under vacuum: green solid (526 mg, 69%). Mp 178 °C. IR (KBr disk): 3495, 3377, 3198, 2970, 2918, 2873, 1610, 1516, 1484, 1444, 1234, 1217, 1049, 823, 768, 579, 510 cm^{-1}. Magnetic moment: 1.78 B.M. Elemental analysis calculated (%) for $C_{13}H_{16}N_2Cl_2O_2Cu$: C 42.58, H 4.40, N 7.64. Found: C 42.66, H 4.39, N 7.30 (X-ray crystallography, see section 4.1-ESI†).

***cis*-Dichloro(*N*-{[4-(2,3,4,6-tetra-*O*-acetyl-β-D-glucopyranosyloxy)pheny]lmethyl}-2-pyridinemethamino)copper (3b).** Compound **2b** (294 mg, 0.54 mmol) was dissolved in ethanol (10 mL) at rt and was added to a solution of $CuCl_2{\cdot}2H_2O$ (110 mg, 0.65 mmol) in ethanol (10 mL). The reaction was allowed to stir overnight. The resulting green solution was allowed to stand for 3 days. A green precipitate formed and was collected by vacuum filtration. This was washed with cold ethanol and dried under vacuum: green solid (216 mg, 59%). Mp 146–147 °C. IR (KBr disk): 3456, 3233, 2998, 2941, 2887, 1753, 1628, 1610, 1512, 1486, 1447, 1431, 1376, 1231, 1045, 908, 769, 600 cm^{-1}. Magnetic susceptibility: 1.81 B.M. Elemental analysis calculated (%) for $C_{27}H_{32}N_2Cl_2O_{10}Cu$: C 47.76, H 4.75, N 4.13. Found: C 47.46, H 4.85, N 3.82.

Bis(*N*-[4-(hydroxyphenyl)methyl]-2-pyridinemethamino)zinc perchlorate monohydrate (4). To a solution of *N*-[4-(hydroxyphenyl)methyl]-2-pyridinemethamine **2a** (397 mg, 1.8 mmol) in ethanol (10 mL) was added a solution of $Zn(ClO_4)_2{\cdot}6H_2O$ (229 mg, 0.6 mmol) in ethanol (10 mL) at rt to immediately yield a beige precipitate. This was stirred for 5 h and the precipitate was collected by vacuum filtration to yield a hygroscopic brown solid. This was then lyophilized for 48 h to yield the product: beige solid (lyophilized after filtration, 207 mg, 62%). Mp: 161–163 °C. ^{1}H NMR (500 MHz, $CDCl_3$) δ 8.11 (bs 1H) 8.03 (bs, 1H), 7.49 (bs, 1H), 7.09 (bs, 2H), 6.77 (bs, 2H, Ar–H), 3.91 (s, 2H, Pyr-CH_2), 3.64 (Ar–CH_2). ^{13}C NMR (126 MHz, DMSO) δ 157.1 (Pyr-C), 148.1 (Ar–C), 147.3 (Pyr-CH), 140.4 (Pyr-CH), 130.5 (Pyr-CH), 130.2 (Ar–C), 124.1 (Ar–CH), 115.7 (Ar–CH), 56.6 (CH_2), 52.0 (CH_2). IR (KBr disk): 3430, 2935, 2968, 1613, 1574, 1517, 1489, 1446, 1375, 1269, 1222, 1177, 1108, 1051, 928, 833, 764, 623, 509 cm^{-1}. Elemental analysis calculated (%) for $C_{26}H_{30}N_4Cl_2O_{11}Zn$: C 43.93, H 4.25, N 7.88. Found: C 44.02, H 4.49, N 8.20.

2-Hydroxy-4-[2-(2,3,4,6-tetra-*O*-acetyl-β-D-glucopyranosyloxy) ethoxy]benzaldehyde (5d). To a solution of 2-chloroethyl 2,3,4,6-tetra-*O*-acetyl-β-D-glucopyranoside[53] (1 g, 2.4 mmol) and sodium iodide (359 mg, 2.4 mmol) in anhydrous acetonitrile (15 mL) was added a solution of 2,4-dihydroxybenzaldehyde (660 mg, 4.8 mmol) and DBU (0.359 mL, 2.4 mmol) in anhydrous acetonitrile (10 mL). The mixture was sealed in a microwave tube under argon and heated under microwave irradiation to 125 °C for 4 h. The solvent was then removed *in vacuo* and the residue was dissolved in dichloromethane (20 mL) and washed with water (2 × 20 mL), aq. $Na_2S_2O_4$ 1 M solution (20 mL), aq. $NaHCO_3$ saturated solution (2 × 20 mL), brine (20 mL) and dried (Na_2SO_4). The solvent was removed in the rotatory evaporator to yield a brown oil which was purified by column chromatography (3 : 1 petroleum ether/ethyl acetate, R_f: 0.17): dark yellow oil (862 mg, 66%). ^{1}H NMR (500 MHz, $CDCl_3$) δ 11.39 (s, 1H, OH), 9.67 (s, 1H, HC═O), 7.40 (d, J = 8.7 Hz, 1H, Ar–H), 6.49 (dd, J = 8.7, 2.3 Hz, 1H, Ar–H), 6.36 (d, J = 2.3 Hz, 1H, Ar–H), 5.18 (t, J = 9.6 Hz, 1H, H-3), 5.05 (t, J = 9.7 Hz, 1H, H-4), 4.97 (dd, J = 9.6, 8.0 Hz, 1H, H-2), 4.61 (d, J = 8.0 Hz, 1H, H-1), 4.22 (dd, J = 12.3, 4.7 Hz, 1H, H-6), 4.16–4.05 (m, 4H, H-6′,OC*H*, CH_2Cl), 3.91 (dt, J = 9.6, 3.5 Hz, 1H, OC*H*′), 3.69 (ddd, J = 9.7, 4.7, 2.4 Hz, 1H, H-5), 2.03, 1.98, 1.95, 1.91 (each s, 3H, OAc). ^{13}C NMR (126 MHz, $CDCl_3$) δ 194.4 (HC═O), 170.6, 170.2, 169.4, 169.3 (each C═O), 165.7 (Ar–C), 164.4(Ar–C), 135.4 (Ar–CH), 115.4 (Ar–C), 108.4 (Ar–CH), 101.3(Ar–CH), 101.0 (C-1), 72.7 (C-3), 71.9 (C-5), 71.1 (C-4), 68.3 (C-2), 67.7 (C-6), 67.4 (CH_2OAr), 61.8 (OCH_2), 20.7, 20.6, 20.5, 20.5 (each OAc). IR (KBr disk): 3471, 2967, 1745, 1633, 1581, 1430, 1379, 1230, 1123, 1044, 989 cm^{-1}. HRMS (ESI+): m/z calculated for $C_{23}H_{29}O_{13}$ + H^+ [M + H^+]: 513.1608. Found: 513.1609. $[\alpha]_D^{25}$: −0.11° (c 1, methanol).

General procedure for imine ligand synthesis (N_2O series)

2-Picolylamine and the corresponding aldehyde (1 equiv.) were dissolved in ethanol (~0.3 M). The reaction mixture was allowed to stir at rt until TLC analysis showed disappearance of the starting material (~4–6 h). The solvent was reduced by half in a rotatory evaporator and cooled on ice to enhance precipitation if required. The precipitate was collected by filtration, washed with cold ethanol and dried under vacuum.

4-{[(2-Methylpyridinyl)-*E*-imino]methyl}-benzene-1,3-diol (6a). Yellow solid (3.12 g, 95%). Mp: 159–160 °C. ^{1}H NMR (500 MHz, $CDCl_3$) δ 8.60 (d, J = 4.9 Hz, 1H, Pyr-H), 8.25 (s, 1H, C(═N)H), 7.77 (dd, J = 8.5, 6.9 Hz, 1H, Pyr-H), 7.42 (d, J = 7.8 Hz, 1H, Pyr-H), 7.35–7.26 (m, 1H, Pyr-H), 6.87 (d, J = 8.4 Hz, 1H, Ar–H), 6.29 (d, J = 2.2 Hz, 1H, Ar–H), 6.20 (dd, J = 8.4, 2.2 Hz, 1H, Ar–H), 4.83 (s, 2H, CH_2). ^{13}C NMR (126 MHz, $CDCl_3$) δ 166.1 (Ar–C), 164.2 (Ar–C), 161.1 (C═N), 157.7 (Pyr-C), 148.9 (Pyr-CH), 137.8 (Pyr-CH), 133.4 (Ar–CH), 123.2 (Pyr-CH), 123.0 (Pyr-CH), 112.3 (Ar–C), 107.3 (Ar–CH), 103.3 (Ar–CH), 63.9 (CH_2). IR (KBr disk): 3435, 3064, 2763, 2676, 2618, 1621, 1442, 1331, 1271, 1120 cm^{-1}. HRMS (ESI+): m/z calculated for $C_{13}H_{12}N_2O_2$ [M^+]: 228.0899. Found. 228.0905. Elemental analysis calculated (%) for $C_{13}H_{12}N_2O_2$: C 68.41, H 5.30, N 12.27. Found: C 68.63, H 5.44, N 12.28 (X-ray crystallography, see section 4.2-ESI†).

5-(2,3,4,6-Tetra-*O*-acetyl-β-D-glucopyranosyloxy)-2-{[(2-methylpyridinyl)-*E*-imino]methyl}phenol (6b). Orange solid (1.12 g, 95%). Mp: 77–78 °C. ^{1}H NMR (500 MHz, $CDCl_3$) δ 13.72 (s, 1H, OH), 8.58 (d, J = 4.9 Hz, 1H, Pyr-H), 8.45 (s, 1H, C(H)═N), 7.69 (td, J = 7.8, 1.9 Hz, 1H, Pyr-H), 7.34 (d, J = 7.8 Hz, 1H, Pyr-H), 7.21 (m, 2H, Pyr-H, Ar–H), 6.56 (d, J = 2.3 Hz, 1H, Ar–H), 6.50 (dd, J = 8.5, 2.3 Hz, 1H, Ar–H), 5.36–5.20 (m, 2H, H-1, H-2), 5.14 (m, 2H, H-3, H-4), 4.91 (s, 2H, CH_2-Pyr), 4.29 (dd, J = 12.3, 5.7 Hz, 1H, H-6), 4.18 (dd, J = 12.3, 2.3 Hz, 1H, H-6′), 3.89 (ddd, J = 10.1, 5.7, 2.3 Hz, 1H, H-5), 2.10, 2.07, 2.05, 2.04 (each s, 3H, OAc). ^{13}C NMR (126 MHz, $CDCl_3$) δ 170.8, 170.3, 169.5, 169.4 (each C═O), 165.9 (C═N), 163.8 (Pyr-C), 160.2 (Ar–C), 157.9 (Ar–C), 149.6 (Pyr-CH), 137.0 (Pyr-CH), 132.9 (Ar–CH), 122.5 (Pyr-CH), 122.0 (Pyr-CH), 114.6 (Ar–C), 108.2 (Ar–CH), 104.2 (Ar–CH), 98.3 (C-1), 72.8 (C-2), 72.3 (C-3), 71.1 (C-5), 68.3 (C-4), 64.6 (CH_2-Pyr), 61.9 (C-6), 20.8, 20.7, 20.7, 20.7 (each OAc). IR (KBr disk): 3472, 3053, 3017, 2965, 2870, 1749, 1635, 1589, 1505, 1368, 1255, 1227, 1176, 1079, 1056, 749 cm^{-1}. HRMS (ESI+): m/z calculated for $C_{27}H_{30}N_2O_{11}$ + H^+ [M + H^+]: 559.1928. Found: 559.1895. $[\alpha]_D^{23}$: −0.23° (c 2, dichloromethane). Elemental analysis calculated (%) for $C_{27}H_{30}N_2O_{11}$: C 58.06, H 5.41, N 5.02. Found: C 58.24, H 5.42, N 5.25.

5-(2-Hydroxyethoxy)-2-{[(2-methylpyridinyl)-*E*-imino]methyl} phenol (6c). Yellow solid (1.22 g, 86%). Mp: 124 °C. ^{1}H NMR (500 MHz, $CDCl_3$) δ 13.83 (s, 1H, Ar-OH), 8.58 (d, J = 4.9 Hz, 1H, Pyr), 8.41 (s, 1H, C(═N)H), 7.69 (td, J = 7.7, 1.8 Hz, 1H, Pyr), 7.35 (d, J = 7.7 Hz, 1H, Ar–H), 7.22–7.20 (m, 1H, Ar–H), 7.18 (d, J = 8.9 Hz, 1H, Ar–H), 6.46 (m, 2H, Ar–H), 6.44 (d, J = 2.4 Hz, 1H, Ar–H), 4.89 (s, 2H, Pyr-CH_2), 4.18–4.06 (t, J = 4.9 Hz, 2H, ArO–CH_2), 4.01–3.92 (t, J = 4.9 Hz, 2H, CH_2OH). ^{13}C NMR (126 MHz, $CDCl_3$) δ 165.8 (C═N), 164.5 (Ar–C), 162.6 (Ar–C), 158.1 (Pyr-C), 149.4 (Pyr-CH), 136.9 (Pyr-CH), 132.9 (Ar–CH), 122.4 (Pyr-CH), 121.9 (Pyr-CH), 112.9 (Ar–C), 106.8 (Ar–CH), 101.9 (Ar–CH), 69.3 ($ArOCH_2$), 64.2 (Pyr-CH_2), 61.3 (CH_2OH). IR (KBr disk): 3406, 3269, 2943, 2927, 2896, 1630, 1596, 1179.5, 1138, 1096, 1044, 844, 763, 614 cm^{-1}. HRMS

(ESI+): *m*/*z* calculated for $C_{15}H_{16}N_2O_3$ + H^+ [M + H^+]: 273.1239. Found: 273.1233. Elemental analysis calculated (%) for $C_{15}H_{14}N_2O_3$: C 66.54, H5.92, N 10.29. Found: C 66.35, H 6.05, N 10.26 (X-ray crystallography, see section 4.3-ESI†).

5-[2-(2,3,4,6-Tetra-*O*-acetyl-β-D-glucopyranosyloxy)ethoxy]-2-{[(2-methylpyridinyl)-*E*-imino]methyl}phenol (6d). Pale yellow solid (1.13 g, 78%). Mp: 118–119 °C. ^{1}H NMR (500 MHz, $CDCl_3$) δ 13.80 (s, 1H, Ar-OH), 8.58 (d, J = 4.0 Hz, 1H, Pyr-H), 8.41 (s, 1H, C(H)═N), 7.69 (td, J = 7.7, 1.8 Hz, 1H, Pyr-H), 7.35 (d, J = 7.8 Hz, 1H, Pyr-H), 7.21 (dd, J = 7.0, 5.4 Hz, 1H, Pyr-H), 7.19–7.14 (m, 1H, Ar–H), 6.44–6.39 (m, 2H, Ar–H), 5.22 (t, J = 9.6 Hz, 1H, H-3), 5.10 (t, J = 9.7 Hz, 1H, H-4), 5.02 (dd, J = 9.6, 8.0 Hz, 1H, H-2), 4.89 (s, 2H, CH_2-Pyr), 4.66 (d, J = 8.0 Hz, 1H, H-1), 4.27 (dd, J = 12.3, 4.7 Hz, 1H, H-6), 4.19–4.06 (m, 4H, H-6′, OCH_2CH_2OAr, $OCHCH_2OAr$), 4.01–3.86 (m, 1H, $OCH'CH_2OAr$), 3.72 (ddd, J = 10.1, 4.7, 2.4 Hz, 1H, H-5), 2.08, 2.03, 2.00, 1.96 (each s, 3H, OAc). ^{13}C NMR (126 MHz, $CDCl_3$) δ 170.8, 170.4, 169.5, 169.5 (each C═O), 165.8 (C═N), 164.5 (Ar–C), 162.5 (Ar–C), 158.2 (Pyr-C), 149.5 (Pyr-CH), 136.9 (Pyr-CH), 133.1 (Ar–CH), 122.5 (Pyr-CH), 121.9 (Pyr-CH), 112.9 (Ar–C), 106.8 (Ar–CH), 101.8 (Ar–CH), 101.2 (C-1), 72.8 (C-3), 72.0 (C-5), 71.2 (C-2), 68.4 (C-4), 68.1 (CH_2OAr), 67.2 (OCH_2), 64.2 (CH_2-Pyr), 61.9 (C-6), 20.8, 20.7, 20.7, 20.7 (each OAc). IR (KBr disk): 3438, 2964, 2935, 2885, 1744, 1630, 1591, 1518, 1433, 1370, 1254, 1224, 1178, 1141, 1093, 1046, 981, 846, 606 cm^{-1}. HRMS (ESI+): *m*/*z* calculated for $C_{29}H_{34}N_2O_{12}$ + H^+ [M + H^+]: 603.2190. Found: 603.2177. $[\alpha]_D^{23}$: −0.16° (*c* 2, dichloromethane). Elemental analysis calculated (%) for $C_{29}H_{34}N_2O_{12}$: C 57.80, H 5.69, N 4.65. Found: C 58.04, H 5.68, N 4.65.

General procedure for metal complexation (N_2O series)

The imino ligand was dissolved in ethanol (~2 M) and added to a solution of the corresponding salt (0.5 equiv. for **7**, 1 equiv. for **8**, ~2 M) in ethanol. The reaction mixture was allowed to reflux for 5 h (for complex **7**) or 3 h (for complex **8**) under nitrogen. The solvent was reduced by half in a rotatory evaporator and cooled on ice to enhance precipitation. The precipitate was collected by filtration, washed with cold ethanol and dried under vacuum.

Aqua(5-hydroxy-2-{[(2-methylpyridinyl)-*E*-imino]methyl}phenoate)copper perchlorate dihydrate (7). Green solid (158 mg, 40%). Mp: 189–191 °C. IR (KBr Disk): 3454, 3208, 3121, 2938, 2913, 2021, 1636, 1615, 1541, 1490, 1334, 1231, 1170, 1057, 625 cm^{-1}. Magnetic susceptibility: 1.77 B.M. Elemental analysis calculated (%) for $C_{13}H_{23}N_2ClO_9Cu$: C 35.14, H 3.86, N 6.31. Found: C 34.96, H 3.75, N 6.79.

(5-Hydroxy-2-{[(2-methylpyridinyl)-*E*-imino]methyl}phenolate) zinc perchlorate monohydrate (8). Yellow solid (859 mg, 65%, stored under argon). Mp: 107–109 °C. ^{1}H NMR (500 MHz, CD_3CN) δ 8.52 (bs, 2H Pyr-H, HC(═N)), 8.11 (bs, 1H, Pyr-H), 7.61 (bs, 2H, Pyr-H), 7.44 (bs, 1H Ar–H), 6.60 (bs, 2H, Ar–H), 5.08 (bs, 2H, CH_2), 3.81 (bs, H_2O, OH). IR (KBr disk): 3437, 3335, 3278, 3090, 2954, 2011, 1611, 1589, 1489, 1439, 1381, 1293, 1089, 1027, 625 cm^{-1}. Mp: 107–109 °C Elemental analysis calculated (%) for $C_{13}H_{15}N_2ClO_8Zn$: C 38.07, H 3.20, N 8.65. Found: C 37.89, H 3.31, N 8.40. A satisfactory ^{13}C NMR spectrum could not to be obtained due to the hydrolysis of the compound over the time scale necessary to obtain the data.

Bis(2-picolylamine)zinc perchlorate (9). $Zn(ClO_4)_2{\cdot}6H_2O$ (723 mg, 1.9 mmol) and 2-picolylamine (0.4 mL, 3.8 mmol) were stirred at rt in ethanol (20 mL) for 4 h and cooled on ice for 30 min. This yielded a white precipitate which was collected by vacuum filtration, washed with cold ethanol and dried under vacuum: white solid (855 mg, 94%). Mp: Compound decomposes at 245 °C. ^{1}H NMR (500 MHz, DMSO) δ 8.30 (d, J = 2.9 Hz, 2H, Pyr-H), 8.05 (t, J = 7.2 Hz, 2H, Pyr-H), 7.59 (d, J = 7.9 Hz, 2H, Pyr-H), 7.56–7.50 (m, 2H, Pyr-H), 4.08 (s, 4H, CH_2), 3.91 (s, 4H, NH_2).^{13}C NMR (126 MHz, DMSO) δ 157.4 (Pyr-C), 146.8 (Pyr-CH), 139.7 (Pyr-CH), 123.8 (Pyr-CH), 123.5 (Pyr-CH), 42.6 (CH_2). IR (KBr disk): 3439, 3281, 3204, 3133, 2912, 1603, 1590, 1569, 1487, 1439, 1383, 1334, 1294, 1141, 1114, 1090, 1032, 1017, 940, 772, 636, 626 cm^{-1}. Elemental analysis calculated (%) for $C_{12}H_{16}N_4Cl_2O_8Zn$: C 29.99, H 3.36, N 11.6. Found: C 29.51, H, 3.32, N 11.45.

Biological assays

Cultivation of mammalian cells. The LLC-MK_2 epithelial cells and RAW 264.7 murine macrophages were maintained in Dulbecco's modified Eagle's medium (DMEM) supplemented with 10% of fetal bovine serum (FBS) at 37 °C in an atmosphere containing 5% CO_2.

Murine macrophage viability assay. The effect of each compound on RAW 264.7 murine macrophages viability was evaluated by MTT assay. Firstly, macrophage cells (10^5 mL^{-1}) were allowed to adhere in 96-well tissue culture plates for 24 h at 37 °C, in a 5% CO_2 atmosphere. Non-adherent cells were removed by washes with PBS and the wells refilled with DMEM medium supplemented with 10% FBS. The macrophages were then incubated with increasing concentration of the test compounds (0.39 to 400 μM) and incubated for additional 24 h at 37 °C, in a 5% CO_2 atmosphere. Subsequently, the culture medium was discharged and the formation of formazan was measured by adding MTT (5 mg mL^{-1} in PBS, 50 μg per well) and incubating the wells for 3 h in the dark at 37 °C. The plates were subsequently centrifuged at 1300 rpm for 8 minutes, the supernatant was removed, the pellet was dissolved in 200 mL of DMSO and the absorbance measured in an ELISA reader at 570 nm (Bio-Tek Instruments). The 50% cytotoxicity inhibitory concentration (CC_{50}) was determined by linear regression analysis.

Parasites and cultivation. Tissue culture trypomastigote forms of *T. cruzi* Y strain, which was isolated from a human case, were obtained from the supernatants of infected LLC-MK_2 epithelial cells after 5 days of incubation in DMEM supplemented with 2% heat-inactivated fetal bovine serum (FBS) at 37 °C in a humidified 5% CO_2. *L. amazonensis* (Josefa strain) promastigotes were maintained by weekly transfers in 25 cm^3 culture flasks with Schneider's insect medium, pH 7.0, supplemented with 10% FBS at 28 °C.

***T. cruzi* viability.** The effects of the compounds (Fig. 1) on *T. cruzi* trypomastigotes were assessed by incubation of the

parasites in DMEM with 2% heat-inactivated FBS. Briefly, trypomastigotes were counted using a Neubauer chamber and resuspended in fresh medium to a final concentration of 10^6 viable cells per mL. The viability was assessed by motility and lack of Trypan blue staining. Each compound was added to the culture at final concentrations ranging from 0.1 to 50 μM. After incubation for 24 h at 37 °C, the number of motile parasites was quantified under light microscopy. The 50% lethal dose (LD_{50}) was determined after 24 h by linear regression. The simple salts $ZnCl_2$ and $CuCl_2{\cdot}2H_2O$ and dimethylsulfoxide (DMSO) were used as appropriated controls.

***L. amazonensis* viability.** The effects of the compounds (Fig. 1) on *L. amazonensis* promastigotes were assessed by incubation in Schneider's insect medium with 10% FBS at 28 °C. Briefly, promastigotes were counted using a Neubauer chamber and resuspended in fresh medium to a final concentration of 10^5 viable cells per milliliter. The viability was assessed by motility and lack of Trypan blue staining. Each compound was added to the culture at final concentrations ranging from 0.1 to 50 μM. After incubation for 72 h at 28 °C, the number of motile parasites was quantified. The 50% inhibitory concentration (IC_{50}) was determined after 72 h by linear regression analysis. The simple salts $ZnCl_2$ and $CuCl_2$ and DMSO were used as appropriate controls.

***T. cruzi* and *L. amazonensis* morphology.** Light microscopy analysis was performed in order to detect some possible alterations on the morphology of *T. cruzi* trypomastigotes and *L. amazonensis* promastigotes after the treatment with the most efficacious compounds at LD_{50} (or IC_{50}) concentration. In this context, the parasites were washed in phosphate-buffered saline (PBS; 150 mM NaCl, 20 mM phosphate buffer, pH 7.2), fixed with methanol, Giemsa-stained for 1 h and then observed in a Zeiss microscope (Axioplan, Oberkochen, Germany).

***G. mellonella* viability.** Sixth instar larvae of *G. mellonella* (the greater wax moth, which belongs to order Lepidoptera, family Pyralidae) were obtained from The Mealworm Company (Sheffield, England) and stored in wood shavings in the dark at 15 °C. Larvae chosen for experiments weighed between 0.17–0.23 g and displayed no discoloration on their cuticle. Five healthy larvae inoculated with each compound and were placed in sterile 9 cm Petri dishes containing a sheet of Whatman filter paper and a small amount of wood shavings. Larvae were incubated at 30 °C and survival was assessed at 24 h and 48 h by response to physical stimulus. Compounds **2a–b**, **3a–b**, **4**, **6a–b**, and **8** were chosen for analysis and were tested at concentrations of 1, 10 and 100 μM. These were administered as solutions in 10% DMSO in PBS buffer by inoculation of the larvae through the last left proleg directly into the hemocoel using a 300 μL Thermo Myjector syringe (29G) with the sterile test solutions (20 μL).

Statistics. All experiments were performed in triplicate, in three independent experimental sets. The data were analyzed statistically by means of Student's *t*-test using EPIINFO 6.04 (Database and Statistics Program for Public Health) computer software. *P* values of 0.05 or less were considered statistically significant.

Acknowledgements

We would like to thank Dr Malachy McCann (Maynooth University) for his advice and guidance and Dr Brendan Twamley (Trinity College Dublin) for his help with X-ray crystallography. We would like to acknowledge Maynooth University for the provision of the John and Pat Hume Scholarship (A. Reddy).

References

1 L. Savioli and D. Daumerie, *Working to overcome the global impact of neglected tropical diseases*, World Health Organization, Geneva, Switzerland, 2010.
2 A. Cavalli and M. L. Bolognesi, *J. Med. Chem.*, 2009, **52**, 7339–7359.
3 I. Silva-Jardim, O. H. Thiemann and F. F. Anibal, *J. Braz. Chem. Soc.*, 2014, **25**, 1810–1823.
4 J. Bermudez, C. Davies, A. Simonazzi, J. Pablo Real and S. Palma, *Acta Trop.*, 2016, **156**, 1–16.
5 J. A. Urbina, *Acta Trop*, 2010, **115**, 55–68.
6 C. Bern, S. P. Montgomery, B. L. Herwaldt, A. Rassi Jr., J. A. Marin-Neto, R. O. Dantas, J. H. Maguire, H. Acquatella, C. Morillo, L. V. Kirchhoff, R. H. Gilman, P. A. Reyes, R. Salvatella and A. C. Moore, *J. Am. Med. Assoc.*, 2007, **298**, 2171–2181.
7 V. Delespaux and H. P. de Koning, *Drug Resist. Updates*, 2007, **10**, 30–50.
8 M. T. Bahia, F. Diniz Lde and V. C. Mosqueira, *Expert Opin. Invest. Drugs*, 2014, **23**, 1225–1237.
9 A. S. Nagle, S. Khare, A. B. Kumar, F. Supek, A. Buchynskyy, C. J. Mathison, N. K. Chennamaneni, N. Pendem, F. S. Buckner, M. H. Gelb and V. Molteni, *Chem. Rev.*, 2014, **114**, 11305–11347.
10 J. Alvar, I. D. Vélez, C. Bern, M. Herrero, P. Desjeux, J. Cano, J. Jannin and M. den Boer, *PLoS One*, 2012, **7**, e35671.
11 P. Desjeux, *Comp. Immunol. Microbiol. Infect. Dis.*, 2004, **27**, 305–318.
12 I. L. Wong, K. F. Chan, T. H. Chan and L. M. Chow, *J. Med. Chem.*, 2012, **55**, 8891–8902.
13 A. Ponte-Sucre, E. Diaz and M. Padrón-Nieves, *Drug Resistance in Leishmania Parasites*, Springer, Vienna, 2013.
14 J. N. Sangshetti, F. A. K. Kahan, A. A. Kulkarni, R. Arote and R. H. Patil, *RSC Adv.*, 2015, **5**, 32376–32415.
15 D. O. Santos, C. E. Coutinho, M. F. Madeira, C. G. Bottino, R. T. Vieira, S. B. Nascimento, A. Bernardino, S. C. Bourguignon, S. Corte-Real, R. T. Pinho, C. R. Rodrigues and H. C. Castro, *Parasitol. Res.*, 2008, **103**, 1–10.
16 S. Khare, A. S. Nagle, A. Biggart, Y. H. Lai, F. Liang, L. C. Davis, S. W. Barnes, C. J. N. Mathison, E. Myburgh, M.-Y. Gao, J. R. Gillespie, X. Liu, J. L. Tan, M. Stinson, I. C. Rivera, J. Ballard, V. Yeh, T. Groessl, G. Federe, H. X. Y. Koh, J. D. Venable, B. Bursulaya, M. Shapiro,

P. K. Mishra, G. Spraggon, A. Brock, J. C. Mottram, F. S. Buckner, S. P. S. Rao, B. G. Wen, J. R. Walker, T. Tuntland, V. Molteni, R. J. Glynne and F. Supek, *Nature*, 2016, **537**, 229–233.
17 K. D. Mjos and C. Orvig, *Chem. Rev.*, 2014, **114**, 4540–4563.
18 R. W. Brown and C. J. T. Hyland, *MedChemComm*, 2015, **6**, 1230–1243.
19 E. Rodríguez-Arce, M. F. Mosquillo, L. Pérez-Díaz, G. A. Echeverría, O. E. Piro, A. Merlino, E. L. Coitiño, C. Maríngolo-Ribeiro, C. Q. F. Leite, F. R. Pavan, L. Otero and D. Gambino, *Dalton Trans.*, 2015, **44**, 14453–14464.
20 E. Iniguez, A. Sanchez, M. A. Vasquez, A. Martinez, J. Olivas, A. Sattler, R. A. Sanchez-Delgado and R. A. Maldonado, *J. Biol. Inorg. Chem.*, 2013, **18**, 779–790.
21 Y. C. Ong, V. L. Blair, L. Kedzierski, K. L. Tucka and P. C. Andrews, *Dalton Trans.*, 2015, **44**, 18215–18226.
22 C. R. Maldonado, C. Marin, F. Olmo, O. Huertas, M. Quiros, M. Sanchez-Moreno, M. J. Rosales and J. M. Salas, *J. Med. Chem.*, 2010, **53**, 6964–6972.
23 A. Martínez, T. Carreon, E. Iniguez, A. Anzellotti, A. Sanchez, M. Tyan, A. Sattler, L. Herrera, R. A. Maldonado and R. A. Sanchez-Delgado, *J. Med. Chem.*, 2012, **55**, 3867–3877.
24 A. B. Caballero, A. Rodriguez-Dieguez, M. Quiros, J. M. Salas, O. Huertas, I. Ramirez-Macias, F. Olmo, C. Marin, G. Chaves-Lemaur, R. Gutierrez-Sanchez and M. Sanchez-Moreno, *Eur. J. Med. Chem.*, 2014, **85**, 526–534.
25 H. Zhang, Y. Ma and X. L. Sun, *Med. Res. Rev.*, 2010, **30**, 270–289.
26 B. Ernst and J. L. Magnani, *Nat. Rev. Drug Discovery*, 2009, **8**, 661–677.
27 C. J. Carroux, G. M. Rankin, J. Moeker, L. F. Bornaghi, K. Katneni, J. Morizzi, S. A. Charman, D. Vullo, C. T. Supuran and S. A. Poulsen, *J. Med. Chem.*, 2013, **56**, 9623–9634.
28 M. Gottschaldt and U. S. Schubert, *Chem. – Eur. J.*, 2009, **15**, 1548–1557.
29 H. Brunner, W. Dafinger and H. Schönenberger, *Inorg. Chim. Acta*, 1989, **156**, 291–301.
30 E. Ferrari, S. Lazzari, G. Marverti, F. Pignedoli, F. Spagnolo and M. Saladini, *Bioorg. Med. Chem.*, 2009, **17**, 3043–3052.
31 A. W. Addison, T. N. Rao, J. Reedijk, J. Vanrijn and G. C. Verschoor, *J. Chem. Soc., Dalton Trans.*, 1984, 1349–1356.
32 A. Okuniewski, D. Rosiak, J. Chojnacki and B. Becker, *Polyhedron*, 2015, **90**, 47–57.
33 L. Yang, D. R. Powell and R. P. Houser, *Dalton Trans.*, 2007, 955–964.
34 T. Chu, L. Belding, P. K. Poddutoori, A. van der Est, T. Dudding, I. Korobkov and G. I. Nikonov, *Dalton Trans.*, 2016, **45**, 13440–13448.
35 M. Sarma and B. Mondal, *Inorg. Chem.*, 2011, **50**, 3206–3212.
36 R. Rowan, C. Moran, M. McCann and K. Kavanagh, *BioMetals*, 2009, **22**, 461–467.
37 M. Salzet, *Trends Immunol.*, 2001, **22**, 285–288.
38 A. P. Desbois and P. J. Coote, *J. Antimicrob. Chemoter.*, 2011, **66**, 1785–1790.
39 J. W. Betts, L. M. Phee, M. H. F. Abdul Momin, K.-D. Umland, J. Brem, C. J. Schofield and D. W. Wareham, *Med. Chem. Commun.*, 2016, **7**, 190–193.
40 B. Demoro, F. Caruso, M. Rossi, D. Benitez, M. Gonzalez, H. Cerecetto, B. Parajon-Costa, J. Castiglioni, M. Galizzi, R. Docampo, L. Otero and D. Gambino, *J. Inorg. Biochem.*, 2010, **104**, 1252–1258.
41 D. A. Martins, L. R. Gouvea, D. da Gama Jean Batista, P. B. da Silva, S. R. Louro, C. S. M. de Nazare and L. R. Teixeira, *BioMetals*, 2012, **25**, 951–960.
42 L. Becco, A. Rodriguez, M. E. Bravo, M. J. Prieto, L. Ruiz-Azuara, B. Garat, V. Moreno and D. Gambino, *J. Inorg. Biochem.*, 2012, **109**, 49–56.
43 D. A. Martins, L. R. Gouvea, G. S. V. Muniz, S. R. W. Louro, D. D. J. Batista, M. D. C. Soeiro and L. R. Teixeira, *Bioinorg. Chem. Appl.*, 2016, **2016**, 11.
44 S. Li, P. A. Crooks, X. Wei and J. de Leon, *Crit. Rev. Toxicol.*, 2004, **34**, 447–460.
45 H. Haase, S. Overbeck and L. Rink, *Exp. Gerontol.*, 2008, **43**, 394–408.
46 A. G. Peniche, A. R. Renslo, P. C. Melby and B. L. Travi, *Antimicrob. Agents Chemother.*, 2015, **59**, 6463–6470.
47 D. R. Rice, P. Vacchina, B. Norris-Mullins, M. A. Morales and B. D. Smith, *Antimicrob. Agents Chemother.*, 2016, **60**, 2932–2940.
48 Y. M. Al-Mulla Hummadi, N. M. Al-Bashir and R. A. Najim, *Ann. Trop. Med. Parasitol.*, 2005, **99**, 131–139.
49 S. J. Turco and A. Descoteaux, *Annu. Rev. Microbiol.*, 1992, **46**, 65–94.
50 M. K. Wassef, T. B. Fioretti and D. M. Dwyer, *Lipids*, 1985, **20**, 108–115.
51 N. Mora-Soumille, S. Al Bittar, M. Rosa and O. Dangles, *Dyes Pigm.*, 2013, **96**, 7–15.
52 J. M. Hu, X. Wang, Y. F. Qian, Y. Q. Yu, Y. Y. Jiang, G. Y. Zhang and S. Y. Liu, *Macromolecules*, 2015, **48**, 5959–5968.
53 A. A. Husain, A. M. Maknenko and K. S. Bisht, *Chem. – Eur. J.*, 2016, **22**, 6223–6227.